Turkish Journal of Physics

Volume 36 | Number 1 Article 8

1-1-2012

Slab waveguide sensor based on amplified phase change due to multiple total internal reflections

SOFYAN A. TAYA

TAHER M. EL-AGEZ

TÜBİTAK

Turk J Phys
36 (2012) , 67 – 76.

doi:10.3906/fiz-1103-23

Slab waveguide sensor based on amplified phase change due to multiple total internal reflections

Sofyan A. TAYA and Taher M. EL-AGEZ
Physics Department, Islamic University of Gaza, P.O. Box 108, Gaza-PALESTINIAN AUTHORITY
e-mail: staya@iugaza.edu.ps, telagez@iugaza.edu.ps

Received: 26.03.2011

Abstract

We present theoretically an optical slab waveguide sensor based on amplified phase change due to multiple total internal reflections (TIRs). Compared with the conventional waveguide sensors, the proposed approach provides higher sensitivity. In this sensor, we adopt the change in the ellipsometric total phase change Δ as the measuring probe of changes in the refractive index (RI) of the cladding. The change in Δ is calculated for large number of alternating total reflections. Numerical calculations show that Δ is strongly dependent on the RI variations of the cladding. Moreover, theoretical simulations show that the resolution of this sensor is predicted to be $\approx 10^{-8}$ refractive index units (RIU). The proposed sensor could be used as a RI and a pressure sensor.

Key Words: Slab waveguides, total internal reflection, Goos Hänchen shift, ellipsometry, uniaxial anisotropic medium, vacuum sensor

1. Introduction

In the last two decades, optical slab waveguides have been of high interest as sensor elements for detection of the refractive indices (RI) of gaseous or liquid samples [1–6]. Various sensing devices based on surface plasmon resonance (SPR) [1–3] and waveguide modes [4–6] have been developed for the measurement of physical, chemical, and biological quantities. The general character of SPR sensors and waveguide mode sensors is that the analyte (material to be detected) is localized in the cladding region and is probed by the evanescent field of the resonance modes. As a result, these devices are called evanescent field sensors. Waveguide mode sensors, based on the technologies of double prism coupling, single prism coupling, and grating coupling, usually consist of a high RI guiding layer sandwiched between a solid substrate and a cladding material. In most cases the substrate has a RI larger than that of the cladding.

A serious drawback of the waveguide mode sensors is that the probe efficiency is relatively limited, since merely a few percent of the mode energy propagates in the cladding. If this percentage could be increased,

probing sensitivity would grow as well. The recent introduction of reverse-symmetry waveguides [7, 8], in which the RI of the substrate is taken to be less than that of the cladding, has changed the situation.

Qi et al [9] has demonstrated a multimode reverse symmetry waveguide sensor based on a prism-coupled free-standing glass plate which was used for the detection of small RI changes in sugar solution. Resolution of order 3×10^{-5} RIU (refractive index units) with a detection range of 1.5×10^{-5} RIU could be reached. Skivesen et al [10] has improved the situation by introducing a grating coupled multimode glass-plate waveguide sensor. The resolution of this sensor varies from 7×10^{-3} to 5×10^{-5} RIU depending on the actual sample RI with a detection range of 0.52 RIU.

In SPR sensors, more than half of the mode energy propagates through the analyte. However, the residual part of the energy propagates through the very lossy metal layer, resulting in a relatively wide resonance dip in the reflectivity. That is why the sensitivity of SPR sensors cannot benefit further from the field enhancement. The detection sensitivity of SPR sensors for the concentration and the RI of samples has been up to the order of 10^{-4} [11].

Dual polarization interferometry (DPI) is another optical waveguide technique that can be used for sensing purposes. It is utilized to probe molecular scale layers adsorbed to the surface of a waveguide by using the evanescent wave of a laser beam confined to the waveguide. It utilizes a waveguide structure that consists of a stack of dielectric layers with reference and sensing layers separated by a layer of cladding that mimics Young's 2-slit experiment in optics [12]. A top dielectric layer is etched to reveal the sensing layer so that two separate channels can be present on a single sensor chip. Light from a laser is passed through the sandwiched waveguide structure and an interference pattern is detected on the opposing side by a CCD camera. One drawback of the DPI is the structure complexity it employs.

In this paper, we propose asymmetrical slab waveguide sensor based on amplified phase change due to multiple total internal reflections (TIRs). A polarized-light source containing both TE and TM polarizations is assumed to propagate in the structure under consideration. The phase shift that the guided wave undergoes due to the propagation in the guiding layer and to the TIR at the film-clad and the film-substrate interfaces is calculated. The phase shift amplification caused by a large number of consecutive zigzag cycles is considered. The variations of the ellipsometric total phase change Δ with the RI of air in the range of 1–1.0005 as well as with the air pressure in the range 0–1500 Torr are studied.

2. Theory

We consider a three-layer slab waveguide as an optical senor. The guiding layer is considered to be uniaxial anisotropic thin film of thickness h and RI of n_f^α, where α denotes the type of polarized illumination: $\alpha =$ s denoting s-polarized light (TE) and $\alpha =$ p denoting p-polarized light (TM). The guiding layer is presumed to be sandwiched between an isotropic cladding and an isotropic substrate of RIs n_c and n_{sub}, respectively. The guides waves are assumed to propagate in z-direction. Helmholtz equation for both polarizations is described by the equation

$$\frac{\partial^2 A_y(x)}{\partial x^2} + k_0^2[n_i^2 - (N^\alpha)^2]A_y(x) = 0, \tag{1}$$

where $A_y(x)$ denotes the $E_y(x)$-field in TE modes and the $H_y(x)$-field in TM modes, while k_0 is the free space wave number. The RI n_i could be either n_c, n_f^α, or n_{sub}, depending on which region we are defining the field in while N^α is the modal RI of the waveguide for α-mode.

The solution of equation (1) in each layer can be written as

$$A_y(x) = a\ e^{-\gamma_c^\alpha (x-h)}\ ,\quad x > h, \tag{2}$$

$$A_y(x) = b_1\ \sin(\gamma_f^\alpha x) + b_2\ \cos(\gamma_f^\alpha x),\quad 0 < x < h, \tag{3}$$

$$A_y(x) = c\, e^{\gamma_{sub}^\alpha x},\quad x < 0, \tag{4}$$

where $\gamma_c^\alpha = k_0\sqrt{(N^\alpha)^2 - n_c^2}$, $\gamma_f^\alpha = k_0\sqrt{(n_f^\alpha)^2 - (N^\alpha)^2}$, and $\gamma_{sub}^\alpha = k_0\sqrt{(N^\alpha)^2 - n_{sub}^2}$.

Using Equations (2)–(4), all the nonvanishing field components can be calculated for the two modes by applying Maxwell's equations. The continuity of the tangential components of the fields gives rise to the characteristic equation which can be written as [13]

$$2\gamma_f^\alpha h + \varphi_c^\alpha + \varphi_{sub}^\alpha = 2m\pi, \tag{5}$$

where m is the mode order and φ_c^α and φ_{sub}^α are the phase shifts that the wave undergoes upon totally reflected at the film-clad and the film-substrate interfaces, respectively. The phase shifts φ_c^α and φ_{sub}^α are given by [13]

$$\varphi_c^s = -2\arctan\left[\sqrt{\frac{(N^s)^2 - n_c^2}{(n_f^s)^2 - (N^s)^2}}\right]\ \text{for TE modes}, \tag{6}$$

$$\varphi_c^p = -2\arctan\left[\left(\frac{n_f^p}{n_c}\right)^2\sqrt{\frac{(N^p)^2 - n_c^2}{(n_f^p)^2 - (N^p)^2}}\right]\ \text{for TM modes}, \tag{7}$$

$$\varphi_{sub}^s = -2\arctan\left[\sqrt{\frac{(N^s)^2 - n_{sub}^2}{(n_f^s)^2 - (N^s)^2}}\right]\ \text{for TE modes}, \tag{8}$$

and

$$\varphi_{sub}^p = -2\arctan\left[\left(\frac{n_f^p}{n_{sub}}\right)^2\sqrt{\frac{(N^p)^2 - n_{sub}^2}{(n_f^p)^2 - (N^p)^2}}\right]\ \text{for TM modes}. \tag{9}$$

It is well known that each mode has discrete values of resonance angles which correspond to the propagation condition. These modal resonance angles are given by

$$\theta_0^\alpha = \sin^{-1}\left[\frac{N^\alpha}{n_f^\alpha}\right]. \tag{10}$$

The waveguide is presumed to be illuminated with a linearly polarized beam containing both p- and s-polarizations at an incidence angle of θ_0 greater than the critical angles of both modes. In order to bring into coincidence the resonance angles for p- and s-polarizations, the condition $\theta_0^s = \theta_0^p = \theta_0$ should be fulfilled. In this situation, the wave inside the core is totally reflected at both interfaces and is confined by the guiding layer in a zigzag path, resulting in a guided mode.

The phase change associated with one period propagation of the zigzag-rays in the guiding layer originates from two sources: reflection at the interfaces and propagation in the guiding medium. The former phase

contribution is given by equations (6)–(9), while the later contribution between two consecutive reflections is given by

$$\beta^{\alpha} = k_0 \frac{h\, n_f^{\alpha}}{\cos\theta_0}. \tag{11}$$

The phase change that the wave undergoes during a complete zigzag cycle for the α-mode is the sum of all contributions and is given by

$$\Phi^{\alpha} = \varphi_c^{\alpha} + \varphi_{sub}^{\alpha} + 2\beta^{\alpha}. \tag{12}$$

We may now calculate the ellipsometric total phase change Δ due to M complete zigzag cycles. We propose a setup composed of; well collimated light source; linear polarizer with its transmission axis makes an angle τ with respect to the plane of incidence; coupling prism; slab waveguide; decoupling prism; rotating analyzer with mechanical angular velocity ω'; convex lens; and a detector, as shown in Figure 1.

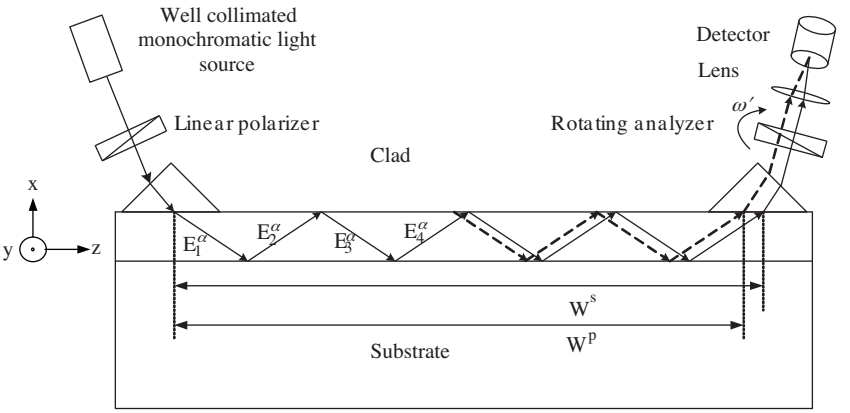

Figure 1. A proposed setup comprising the light source; linear polarizer with its transmission axis at an angle τ with respect to the plane of incidence; coupling prism; slab waveguide; decoupling prism; rotating analyzer with mechanical angular velocityω'; convex lens; and a detector. W^s and W^p are the total lateral displacements covered along the z-direction after performing M zigzag cycles by s- and p-polarized lights, respectively.

If the incident beam just outgoing from the coupling prism to the guiding layer is expressed asE_0^{α}, the successive reflected rays can be expressed by appropriately modifying both the amplitude and the phase of the initial wave. Referring to Figure 1, we can write the time-independent fields as

$$E_1^{\alpha} = r_{sub}^{\alpha} E_0^{\alpha} e^{i\beta^{\alpha}}, \tag{13}$$

$$E_2^{\alpha} = r_c^{\alpha} r_{sub}^{\alpha} E_0^{\alpha} e^{i2\beta^{\alpha}}, \tag{14}$$

$$E_3^{\alpha} = r_{sub}^{\alpha} r_c^{\alpha} r_{sub}^{\alpha} E_0^{\alpha} e^{i3\beta^{\alpha}}, \tag{15}$$

$$E_4^{\alpha} = r_c^{\alpha} r_{sub}^{\alpha} r_c^{\alpha} r_{sub}^{\alpha} E_0^{\alpha} e^{i4\beta^{\alpha}}, \tag{16}$$

and so on, where r_{sub}^{α} and r_c^{α} are the complex Fresnel reflection coefficients for the film-substrate and the film-clad interfaces, respectively. In the case of TIR, they are given by $r_{sub}^{\alpha} = e^{i\varphi_{sub}^{\alpha}}$, $r_c^{\alpha} = e^{i\varphi_c^{\alpha}}$ [14].

Inspection of Equations (13)–(16) shows that E_r^{α} after M such complete cycles can be written as

$$E_r^{\alpha} = E_0^{\alpha} e^{iM(\varphi_c^{\alpha} + \varphi_{sub}^{\alpha} + 2\beta^{\alpha})} = E_0^{\alpha} e^{iM\Phi^{\alpha}}. \tag{17}$$

The reflection coefficient of the whole structure after performing M cycles is given by

$$r^{\alpha} = \frac{E_r^{\alpha}}{E_0^{\alpha}} = e^{iM\Phi^{\alpha}} = e^{i\delta^{\alpha}}. \tag{18}$$

The ellipsometric total amplified phase change between p- and s-polarized lights after performing M cycles is given by [15]

$$\Delta = \delta^p - \delta^s = M(\Phi^p - \Phi^s). \tag{19}$$

If the p- and s-polarizations illuminate the sample simultaneously, the reflected p- and s-fields are related to the incident fields by [16]

$$\begin{pmatrix} E_r^p \\ E_r^s \end{pmatrix} = \begin{pmatrix} r^p r^{ps} \\ r^{sp} r^s \end{pmatrix} \begin{pmatrix} E_0^p \\ E_0^s \end{pmatrix}, \tag{20}$$

where r^{ps} is the amplitude refection coefficient of p-polarized light generated by illumination of the sample by s-polarized light and vice versa for r^{sp} [16]. E_0^p and E_0^s are related to the polarizer azimuth angle τ by

$$E_0^p = E_0 \cos\tau \text{ and } E_0^s = E_0 \sin\tau, \tag{21}$$

where E_0 is the intensity emerging from the polarizer.

The Jones matrix for light reflection becomes diagonal when the optical axis is parallel or perpendicular to the plane of incidence, i.e., $r^{ps} = r^{sp} = 0$ [16].

Consequently, Jones matrix of the system after M zigzag cycles can be written as

$$S = \begin{pmatrix} r^p 0 \\ 0 r^s \end{pmatrix} = \begin{pmatrix} e^{iM\Phi^p} 0 \\ 0 e^{iM\Phi^s} \end{pmatrix}. \tag{22}$$

The transfer matrix for the whole system using Jones formalism can be written as

$$E_t = \begin{pmatrix} \cos^2\omega' t & \sin\omega' t\cos\omega' t \\ \sin\omega' t\cos\omega' t & \sin^2\omega' t \end{pmatrix} \begin{pmatrix} e^{iM\Phi^p} & 0 \\ 0 & e^{iM\Phi^s} \end{pmatrix} \begin{pmatrix} E_0\cos\tau \\ E_0\sin\tau \end{pmatrix}, \tag{23}$$

where E_t is the field of the merging beam at the detector. Hence, the intensity received by the detector is given by $I(t) = E_t^{\dagger} E_t$, i.e.,

$$I(t) = \eta\,[1 + (\cos^2\tau - \frac{1}{2})\cos 2\omega' t + \sin\tau\cos\tau\cos\Delta\sin 2\omega' t], \tag{24}$$

where η is a constant. $I(t)$ may also be written as

$$I(t) = a_0 + a_1\cos 2\omega' t + b_1\sin 2\omega' t, \tag{25}$$

where a_0, a_1, and b_1 are the Fourier coefficients of the intensity $I(t)$ and are given by $a_0 = \eta$, $a_1 = \eta(\cos^2\tau - \frac{1}{2})$, and $b_1 = \eta\sin\tau\cos\tau\cos\Delta$.

The ellipsometric total phase change Δ can be written in terms of Fourier coefficients as

$$\Delta = \cos^{-1}\left(\frac{b_1}{a_0\sin\tau\cos\tau}\right). \tag{26}$$

If the transmission axis of the linear polarizer makes an angle $\tau = 45^\circ$ with respect to the plane of incidence, equation (26) becomes

$$\Delta = \cos^{-1}\left(\frac{2b_1}{a_0}\right). \tag{27}$$

During TIR at the interface separating two media, the reflected light beam undergoes a small lateral shift called the Goos-Hänchen (GH) shift [3, 17], as shown in Figure 2. Such spatial shift is attributed to the evanescent wave that travels along the interface. It appears as if the incident light penetrates first into the lower-refractive-index medium as an evanescent wave before being totally reflected back into the high-index medium. It is well known that the complex reflection coefficient is polarization dependent. Therefore, the resulting GH displacement will also be slightly dependent on the polarization state of the incident beam. GH-shifts, at the film-clad and the film-substrate interfaces, are given by

$$z^s_{GH,i} = \frac{\lambda}{\pi}\frac{\tan\theta_0}{\sqrt{(N^s)^2 - n_i^2}}, \text{ for TE modes,} \tag{28}$$

$$z^p_{GH,i} = \frac{\lambda}{\pi}\frac{\tan\theta_0}{\sqrt{(N^p)^2 - n_i^2}\left[\left(\frac{N^p}{n_f^p}\right)^2 + \left(\frac{N^p}{n_i}\right)^2 - 1\right]}, \text{ for TM modes,} \tag{29}$$

where i denotes "c$''$ at the film-clad interface, or for "sub" at the film-substrate interface.

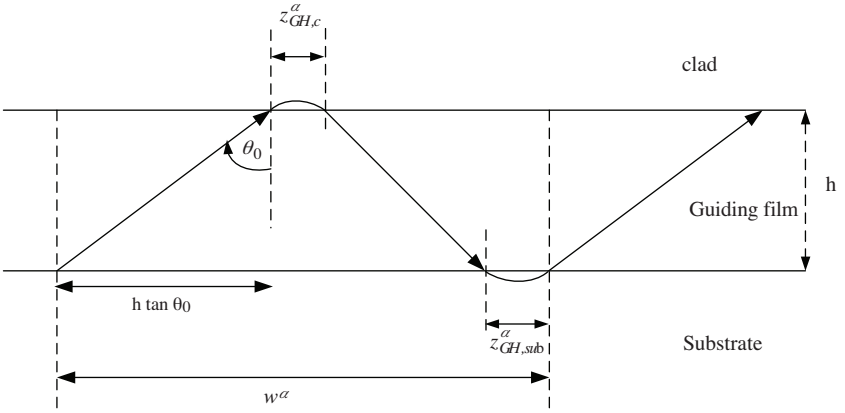

Figure 2. Sketch of light undergoing total internal reflection (TIR). The reflected beam leaves a distance $z^{\alpha}_{GH,c}$ and $z^{\alpha}_{GH,sub}$ along the film-clad and the film-substrate interfaces, respectively. This distance is called Goos-Hänchen shift. w^{α} is the waveguide width corresponds to one period propagation of the zigzag rays in the guiding layer.

The waveguide width w^{α} corresponds to one period propagation of the zigzag rays in the guiding layer is the sum of $2h\tan\theta_0$ and the two Goos-Hänchen lateral shifts at the boundaries of the film as shown in Figure 2, that is

$$w^{\alpha} = 2h\tan\theta_0 + z^{\alpha}_{GH,c} + z^{\alpha}_{GH,sub}. \tag{30}$$

As shown in Figure 1, the total lateral displacement covered along the z-direction after performing M zigzag cycles is given by

$$W^{\alpha} = M\, w^{\alpha}. \tag{31}$$

As mentioned above, this lateral shift is polarization dependent and will cause a spatial spread of the reflected beam along the z-axis particularly if the beam suffers a large number of TIRs. This splitting problem can be solved by introducing a converging lens to focus the two polarized components on the detector.

3. Numerical applications: Air refractive index and pressure sensor

The system under consideration can support multiple modes ($m = 0, 1, 2, \ldots$) and we here consider only the fundamental mode ($m = 0$) due to the high sensitivity of this mode.

It is well known that the modal angle of s-polarization is greater than that of p-polarization for isotropic guiding layer. Therefore, to bring into coincidence the modal angles for p- and s-polarizations, we consider the guiding layer to be a negative uniaxial anisotropic TiO_2 thin film of RIs $n_x = n_z = n_f^p = 3.29$ and $n_y = n_f^s = 2.91$ at the wavelength of 420 nm, at which TiO_2 is lossless [18]. Any wavelength in the region 420 nm $< \lambda <$ 8040 nm can be used since the extinction factor of TiO_2 is zero in this region [18].

The substrate is assumed to be glass of RI of 1.5. The crossover resonance incidence angle for p- and s-polarizations was determined graphically from Figure 3 to be 79.28° at a guiding layer thickness of 363.3 nm. The clad is assumed to have a variable RI which varies from 1 to 1.0005 which corresponds to the RI of vacuum to air at 1500 Torr.

The ellipsometric parameter Δ was calculated for n_c successively varied from 1.0000 to 1.0005 in steps of 10^{-7} while fixing the other variables. The difference between Δ at any value of the considered range of n_c and that at $n_c = 1$ for 2, 100, 400, and 1000 cycles was computed and plotted in Figure 4. As can be seen, for 2 cycles, the change in Δ is barely detectable. As the number of considered cycles increases, this change is amplified. It is about 100° for 1000 cycles. The figure also shows a linear variation of Δ with the RI of the cladding in the range 1.0000 to 1.0005. Assuming a measurable angle resolution of order 0.01°, the resolution of the proposed sensor is of order 5×10^{-8} RIU with a detection range of 5×10^{-4} RIU which is considerably high resolution.

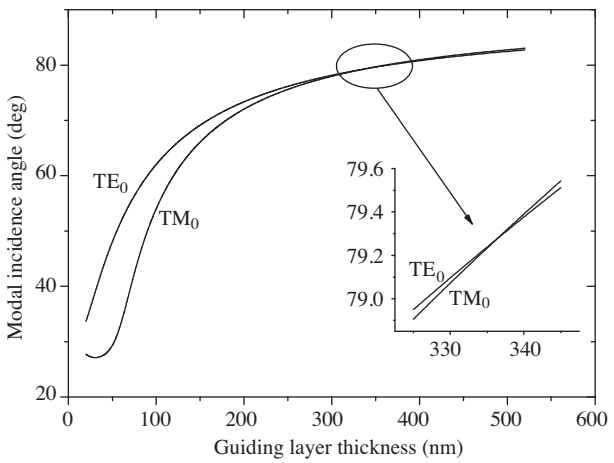

Figure 3. Modal incidence angle for TM_0 and TE_0 polarizations as a function of the guiding layer thickness. The crossover resonance angle is found to be 79.28° at a guiding layer thickness of 363.3 nm.

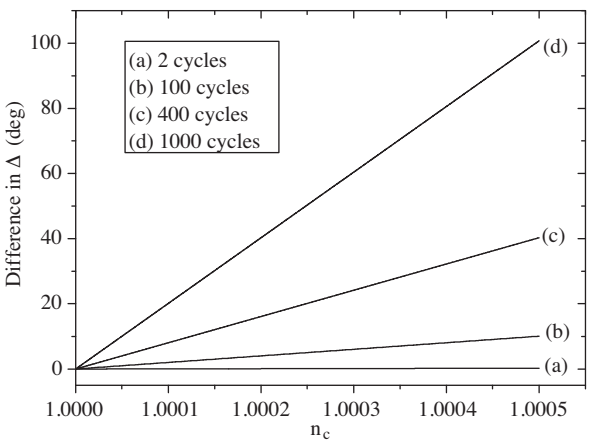

Figure 4. The difference in Δ as a function of the clad refractive index for different number of cycles.

As a practical example, we consider the same example proposed by Horvath et al. in reference [19]. The cladding is assumed to be ultra-pure water ($n_c = 1.331$). The ellipsometric total phase change Δ is calculated using the above set of equations and found to be 69.143°. A pollutant (NaSCN) is assumed to be added to the pure water resulting in 5 wt% NaSCN solution corresponding to a cladding refractive index of 1.342. The parameter Δ is then calculated and found to be 172.72°. Then for a change in n_c of order 0.011, the change in Δ is 103.577°. The high sensitivity of the proposed sensor is obvious.

To demonstrate the feasibility of the proposed sensor in terms of its width, the working width is plotted for different number of cycles in Figure 5 according to equation (31) for TE_0 mode. To evaluate the working width of the proposed sensor for a given number of cycles, it is plotted as a function of the number of cycles using equation (31), as shown in Figure 5. It is found that a width of few millimeters is required, e.g., a width of 4.1 mm is enough for 1000 cycles which is practically acceptable.

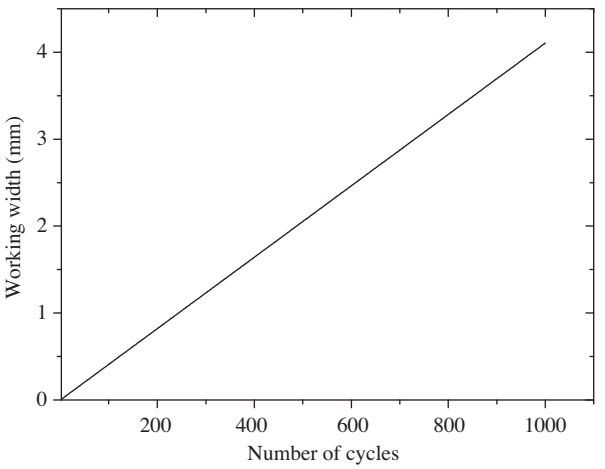

Figure 5. The working width of the proposed sensor versus the number of cycles.

The proposed sensor can be used for example to measure the air pressure for a vacuum chamber or a pressure tube. The variation of the RI of air with pressure is based on the equation [20]

$$n_{air} = 1 + (n_s - 1)\frac{P[1 + P(60.1 - 0.972t)10^{-10}]}{96095.43(1 + 0.003661t)}, \tag{32}$$

where t (°C) is the temperature, P (Pa) is the pressure, and n_s is given by the dispersion equation

$$n_s = \left(8342.54 + \frac{2406147}{(130 - 1/\lambda^2)} + \frac{15998}{(38.9 - 1/\lambda^2)}\right) \times 10^{-8} + 1, \tag{33}$$

where λ is expressed in μm.

In Figure 6, the calculated intensity received by the detector as a function of the analyzer angle for different air pressures is plotted at $t = 27$ °C and $\lambda = 420$ nm. A substantial change in the intensity with the variation of air pressure can be measured. Figure 7 shows the calculated Δ with air pressure from 0–1500 torr for 400 cycles.

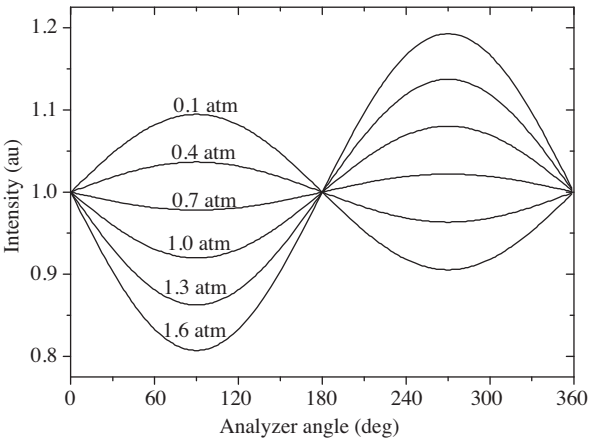

Figure 6. The calculated intensity received by the detector as a function of the analyzer angle for different air pressures.

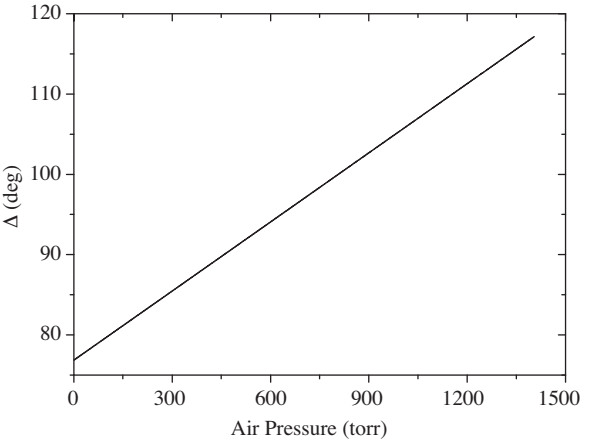

Figure 7. The calculated phase angle Δ as a function of air pressure for 400 reflections.

4. Conclusion

Amplification of phase change due to multiple TIRs is adopted to construct an optical waveguide sensor of high sensitivity compared with the conventional waveguide sensors. The proposed sensor was theoretically applied to measure very small changes in the RI of air. As an example of the use of this sensor, the RI change can be used as an indicator for the change in the pressure of air in a vacuum vessel. We believe that this sensor can compete with the conventional sensors used in this field. Theoretical calculations show that the resolution of this sensor is predicted to be in the order 10^{-8} RIU with a detection range of 5×10^{-4} RIU.

It is well known that electromagnetic waves can be guided for long distances with minimal loss which depends on the quality of the optical materials used. So it is worth to mention that the losses due to absorption and scattering, e.g. due to surface defects, don't have considerable effect on the performance of the device because of the small working width which is on the order of a few millimeters. Moreover, the measured quantity in the proposed device is not the intensity but the difference in overall phase change.

Finally, one important issue should be discussed in some detail: the angle of incidence. The principle of operation of the proposed sensor is based on measuring the difference in amplified phase change between the two light components. Thus, the two components must be coupled into the structure simultaneously. A guided mode can exist only when a transverse resonance condition is satisfied so that the repeatedly reflected wave has constructive interference with itself. The phase shifts caused by internal reflection at a given angle θ depend on the polarization. Therefore, TE and TM waves have different modal incidence angles. If an isotropic guiding layer is used, there is no incidence angle that can make guidance for both polarizations. Anisotropic guiding layer should be used such that a specific and unique incidence angle can make guidance for both components. Practically, nearly parallel beam with small divergence incident at the modal angle can be used to overcome this precise angle condition. The rays of the beam that satisfies the resonance angle condition will be guided while others will be radiated.

References

[1] B. Liedberg, C. Nylander, and I. Lundström, *Sens. Act. B*, **4**, (1983), 299.

[2] P. I. Nikitin, A. A. Beloglazov, M. V. Valeiko, J. A. Creighton, A. M. Smith, N. A. J. M. Sommerdijk, and J. D. Wright, *Sens. Act. B*, **38–39**, (1997), 53.

[3] R. J. Green, R. A. Frazier, K. M. Shakesheff, M. C. Davies, C. J. Roberts, and S. J. Tendler, *Biomaterials*, **21**, (2000), 1823.

[4] T. Okamto, M. Yamomoto, and I. Yamaguchi, *J. Opt. Soc. Am. A*, **17**, (2000), 1880.

[5] D. Qing and I. Yamaguchi, *J. Opt. Soc. Am. B*, **16**, (1999), 1359.

[6] R. Horvath, H. Pedersen, N. Skivesen, D. Selmeczi, and N. B. Larsen, *Opt. Lett.*, **28**, (2003), 1233.

[7] R. Horvath, H. Pederson, and N. Larsen, *App. Phys. Lett.*, **81**, (2002), 2166.

[8] R. Horvath, L. Lindvold, and N. Larsen, *App. Phys. B*, **74**, (2002), 383.

[9] Z. Qi, N. Matsuda, J. Santos, A. Takatsu, and K. Kato, *Opt. Lett.*, **27**, (2002), 689.

[10] N. Skivesen, R. Horvath, and H. Pedersen, *Opt. Lett.*, **28**, (2003), 2473.

[11] K. Matsubara, S. Kawata, and S. Minami, *Appl. Opt.*, **27**, (1988), 1160.

[12] H. N. Daghestani and B. W. Day, *Sensors*, **10,** (2010), 9630.

[13] K. Tiefenthaler and W. Lukosz, *J. Opt. Soc. Am. B*, **6**, (1989), 209.

[14] S. Zhu, A. Yu, D. Hawley, and R. Roy, *Am. J. of Phys.*, **54**, (1986), 601.

[15] R. M. Azzam and N. M. Bashara, Ellipsometry and Polarized Light, (North-Holland, Amsterdam, 1977).

[16] H. Fujiwara, Spectroscopic Ellipsometry Principles and Applications, (John Wiley & Sons, West Sussex, 2007).

[17] F. Goos and H. Hänchen, *Ann. Phys.*, **1**, (1947), 333.

[18] E. D. Palik, Handbook of optical constants of solids, (Academic Press, San Diego, CA, 1998).

[19] R. Horvath, N. Skivensen, and H. C. Pedersen, *Appl. Phys. Lett.*, **84**, (2004), 4044.

[20] K. P. Birch and M. J. Downs, *Metrologia*, **31**, (1994), 315.